



UNIVERSITY OF LEEDS

This is a repository copy of *Molecular Interactions between a Biodegradable Demulsifier and Asphaltenes in an Organic Solvent*.

White Rose Research Online URL for this paper:  
<http://eprints.whiterose.ac.uk/109962/>

Version: Accepted Version

---

**Article:**

Natarajan, A, Kuznicki, N, Harbottle, D et al. (3 more authors) (2016) Molecular Interactions between a Biodegradable Demulsifier and Asphaltenes in an Organic Solvent. *Energy & Fuels*, 30 (12). pp. 10179-10186. ISSN 0887-0624

<https://doi.org/10.1021/acs.energyfuels.6b01889>

---

**Reuse**

Unless indicated otherwise, fulltext items are protected by copyright with all rights reserved. The copyright exception in section 29 of the Copyright, Designs and Patents Act 1988 allows the making of a single copy solely for the purpose of non-commercial research or private study within the limits of fair dealing. The publisher or other rights-holder may allow further reproduction and re-use of this version - refer to the White Rose Research Online record for this item. Where records identify the publisher as the copyright holder, users can verify any specific terms of use on the publisher's website.

**Takedown**

If you consider content in White Rose Research Online to be in breach of UK law, please notify us by emailing [eprints@whiterose.ac.uk](mailto:eprints@whiterose.ac.uk) including the URL of the record and the reason for the withdrawal request.



[eprints@whiterose.ac.uk](mailto:eprints@whiterose.ac.uk)  
<https://eprints.whiterose.ac.uk/>

# Molecular Interactions between a Biodegradable Demulsifier and Asphaltenes in an Organic Solvent

Anand Natarajan<sup>1</sup>, Natalie Kuznicki<sup>1</sup>, David Harbottle<sup>1,2</sup>, Jacob Masliyah<sup>1</sup>, Hongbo Zeng<sup>1\*</sup>,  
Zhenghe Xu<sup>1\*</sup>

1 Department of Chemical and Materials Engineering, University of Alberta, Edmonton, Alberta, T6G 2V4, Canada.

2 School of Chemical and Process Engineering, University of Leeds, Leeds, LS2 9JT, UK.

\*E-mail: [hongbo.zeng@ualberta.ca](mailto:hongbo.zeng@ualberta.ca); phone: 780-492-1044; fax: 780-492-2881; and e-mail: [zhenghe.xu@ualberta.ca](mailto:zhenghe.xu@ualberta.ca); phone: 780-492-7667; fax: 780-492-2881.

## ABSTRACT

A surface forces apparatus (SFA) was used to measure the intermolecular forces between a biodegradable demulsifier (ethyl cellulose, EC) and asphaltenes immobilized on two molecularly smooth mica surfaces in an organic solvent. A steric repulsion on approach between the immobilized EC layers and asphaltenes was measured, despite strong adhesion ( $F_{ad}/R \approx -2 \text{ mN/m}$ ;  $W_{ad} = 0.42 \text{ mJ/m}^2$ ) during retraction. The measured adhesion was attributed to the interpenetration and tangling of aliphatic branches of swollen asphaltenes and solvated chains of EC macromolecules. Competitive adsorption of EC on/in immobilized asphaltene layers was confirmed by combining SFA force measurements and atomic force microscopy (AFM) imaging. Following the injection of EC-in-toluene solution, an immediate (< 5 min) increase in the confined layer thickness of the immobilized asphaltenes layers was measured. Irreversibly adsorbed asphaltenes were displaced by EC macromolecules through binding with unoccupied surface sites on mica, followed by the spreading of EC across the mica substrate due to increased surface activity governed by the higher number of hydroxyl groups per EC molecule. AFM imaging confirmed that the increase in confined layer thickness resulted from the formation of larger asphaltene aggregates/clusters protruding from the mica substrate. Molecular level topographical images showed that the asphaltenes were not re-solvated in the

organic phase but more self-associated as the EC macromolecules spread across the hydrophilic mica substrate. The results from this study provide not only fundamental insights into the basic interaction mechanisms of asphaltenes and EC macromolecules as a demulsifier in organic media, but also directions towards enhancing demulsification of water-in-oil emulsions.

## **Introduction**

The formation of stable emulsions (water-in-oil, oil-in-water, and multiple emulsions) is ubiquitous in the production of crude oil.<sup>1</sup> The mixing of two immiscible liquids in the presence of several interfacially active species creates problematic petroleum emulsions which are difficult to break.<sup>2,3,4</sup> Asphaltenes and fine bi-wettable solid particles (clays) are known to stabilize such emulsions since they readily partition at the liquid-liquid interface to create mechanical barriers that resist droplet coalescence.<sup>5-12</sup> Recent research has shown that the continual accumulation of asphaltenes at the oil-water interface leads to the formation of elastically-dominated interfacial layers that rupture once a critical yield stress is exceeded.<sup>5,13-15</sup> This yield stress is significantly greater than the typical stress applied during droplet-droplet collision;<sup>16,17</sup> as a result, alternative routes have been explored to reduce the rigidity of these interfacial layers.

In the worst case when rag-layers or dense packed layers are formed, oil-water separation is essentially stopped by the presence of excess bi-wettable solids and asphaltenes that resist the density driven migration of oil and/or water droplets.<sup>18,19</sup> To overcome such issues and enhance oil dewatering performance, chemical additives such as dispersants and demulsifiers are typically added at the ppm level to break particle and interfacial networks, thus promoting droplet-droplet coalescence.<sup>20-22</sup>

Chemical demulsifiers are designed to actively compete at the liquid-liquid interface and disrupt the rigid networks which have formed a protective barrier around water droplets.<sup>20,21,23,24</sup> To facilitate their interfacial activity, demulsifier molecules must demonstrate an appreciable level of amphiphilicity to partition at the oil-water interface.<sup>25</sup> Ethylene oxide and propylene oxide

(EO-PO) based polymers have frequently been studied to understand the effects of molecular weight, molecular structure and composition on demulsifier performance.<sup>21,26,27</sup>

Historically, demulsifier performance has been assessed against the reduction in oil-water interfacial tension and/or dilatational modulus.<sup>28,29,30,31</sup> However, these properties are not always satisfactory to describe the effectiveness of demulsifiers, especially the time-dependent dynamics. Recent advances in measurement capability have allowed the mechanical properties of the oil-water interfacial layers and intervening liquid film (asphaltenes partitioned at a water-oil interface) to be probed in real-time as demulsifiers competitively adsorb at the oil-water interface.<sup>21,25,32</sup> The interfacial elasticity as measured under shear has been identified as a key parameter that governs droplet stability.<sup>15</sup> Effective demulsifiers have been shown to reduce the shear elastic contribution of the interfacial layers within seconds following their addition.<sup>33,34</sup> This breakup of a rigid interfacial layer has also been visualised in real-time using a specially designed thin-liquid film force balance technique.<sup>33</sup>

More recently a new biodegradable demulsifier (ethyl cellulose, EC) has been considered to shed light on the demulsification process.<sup>25</sup> Using the micropipette technique, EC was clearly shown to be an effective demulsifier to induce the instantaneous coalescence of water droplets at a critical demulsifier concentration (130 ppm).<sup>20</sup> In the absence of EC, water droplets remain stable to coalescence despite being substantially compressed and rolling around each other as the droplets are brought into contact. At an intermediate EC demulsifier concentration of 35 ppm, water droplets do not coalesce, but significant adhesion and droplet stretching is observed as the two droplets are retracted from contact. While this intermediate chemical dosage is not favorable for coalescence and free-water dropout, water droplet flocculation is a second mechanism to enhance dewatering. The micropipette measurements confirm that interactions between molecular species at the oil-water interface govern the dewatering mechanism. Hence, there is a need to better understand the molecular interactions between competing surface active components, such as asphaltenes and demulsifier molecules.

To advance the mechanistic understanding of demulsification several researchers have applied techniques such as AFM to image asphaltenes/bitumen networks before and after demulsifier addition.<sup>25,35</sup> These interfacial layers have been examined either at the solid-liquid interface (direct imaging) or transferred from a liquid-liquid interface using the Langmuir-Blodgett technique (indirect imaging). Both approaches have demonstrated the generation of large voids in the interfacial layer as the demulsifier molecules begin to occupy more interfacial area. However, the nature of the interaction forces between asphaltenes and demulsifier molecules has never been studied.

Nevertheless asphaltene adsorption at the solid-liquid interface has been studied to better understand the properties of interfacial layers.<sup>36</sup> Interfacial layer formation is frequently described as Langmuir-type, although research using thin-liquid film balance and SFA has shown the formation of multi-layer structures, with an asphaltene layer thickness much greater than the hydrodynamic diameter of asphaltenes in solution.<sup>4,10,37,38</sup> Previous studies have also shown that the adsorption of asphaltenes onto solids (minerals) can significantly enhance the surface hydrophobicity of the particles, and hence increase the ability for particles to partition and stabilize oil-water interfaces. In particular, iron-bearing heavy minerals such as siderite and pyrite have been shown to preferentially partition in the rag layer due to strong binding between carboxylic acids of organic compounds native in crude oil and the heavy minerals.<sup>39</sup> Several recent studies highlighted chemical and structural differences between asphaltenes that strongly adsorb at the oil-water and oil-solid interfaces and those remaining in the bulk oil.<sup>40,41,42</sup> An extended SARA analysis<sup>33</sup> where asphaltenes are fractionated and characterized according to their adsorption affinity confirmed differences between adsorbed asphaltenes and whole asphaltenes. In particular, asphaltenes strongly partitioned at the oil-water interface contain a particularly high oxygen content, which led to the increased presence of sulfoxide groups.<sup>41</sup> Higher oxygen content was also reported for asphaltenes irreversibly adsorbed from oil onto calcium carbonate, accompanied by higher concentrations of carbonyl and carboxylic acid groups.<sup>42</sup> These studies on isolating and characterizing adsorbed asphaltenes have provided a much improved understanding of the most troublesome fractions of asphaltene science.

With chemical demulsifiers often delivered via the organic phase it is important to study interactions of asphaltenes and demulsifier molecules in non-aqueous media via an asymmetrical (asphaltene-EC) system in comparison with symmetrical (asphaltene-asphaltene, EC-EC) systems. A fundamental understanding of the emulsion stabilization mechanism and the subsequent destabilization by demulsifier addition can only be realized through a good description of the interaction forces that act between interfacially active asphaltenes and demulsifier molecules. To that effect, we use in the current study a surface forces apparatus (SFA) to measure the interaction forces ( $F$ ) as a function of surface separation ( $D$ ) between immobilized asphaltenes and EC in an organic solvent. Here we mimic stable interfacial layers by immobilized asphaltenes on mica with EC as the demulsifier. The force profiles obtained from SFA measurements can provide valuable information on material properties such as interaction energies in organic solvent, while AFM imaging was used to provide complementary information on the surface molecular conformation changes of the interacting layers.

## MATERIALS AND EXPERIMENTAL METHODS

**Materials.** Bitumen was kindly provided by Syncrude Canada Ltd. (Alberta) and the asphaltenes were precipitated by adding n-heptane to bitumen at a volume ratio 40:1. A detailed description on asphaltenes precipitation and washing was provided in our previous publication.<sup>38</sup> High-performance liquid chromatography (HPLC) grade toluene and heptane were purchased from Fisher Scientific and used as received. Ethyl cellulose (EC4) was purchased from Sigma-Aldrich and used without further purification. The molecular structure of ethyl cellulose is shown in Figure 1. Although EC is a linear polymer, its molecular chain contains many six-member-ring repeating units connected to each other by a single oxygen atom. The hydroxyl and oxyethyl side groups are either equatorial or axial, located on both sides of the ring.<sup>25</sup> Ruby mica sheets were purchased from S & J Trading Inc. (Glen Oaks, NY) and used as the substrate for immobilizing asphaltenes and/or EC.

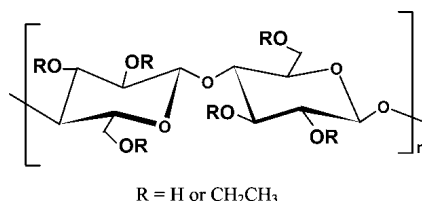


**Figure 1.** Molecular structure of ethyl cellulose (EC).<sup>25</sup>

**Sample Preparation.** The sample preparation method was varied according to the experimental setup. Asphaltene/EC layers were immobilized on mica surfaces by dip coating method. Briefly, after gluing a freshly cleaved thin mica sheet on a cylindrical silica disk, several drops of 0.5 wt% asphaltene- or EC-in-toluene solution were placed and spread on the top surface of the glued mica in a chamber saturated with toluene. The solution was left in contact with mica surfaces for ~15 min to allow a layer of asphaltene or EC to adsorb/assemble on the mica. The sample was then washed with ample amount of pure toluene and blow-dried with particle-free nitrogen before it was loaded in the SFA chamber. The dip-coated mica surfaces are referred to as immobilized layers. The immobilized layers were imaged by AFM and the interaction forces were measured using SFA. Alternatively, 0.5 wt% EC-in-toluene solution was injected in-between two molecularly smooth mica surfaces loaded in the SFA chamber. The adsorption of EC from the bulk solution to mica was monitored in real time by SFA. The surface layer obtained as such is referred to as adsorbed layer to distinguish the immobilized layers which were dried to force the molecules further bind to the solid surfaces and among themselves before force measurement.

**Force Measurement.** SFA was used to measure the molecular interaction forces between EC and asphaltene layers immobilized or adsorbed on mica surfaces. Detailed description on the SFA experiments has been reported elsewhere.<sup>43,44</sup> Briefly, thin mica sheets (1-5  $\mu\text{m}$  thick) were coated with a ~50 nm semi reflective layer of silver on the back surface. The silver coating is required to obtain sharp multiple beam interference fringes of equal chromatic order (FECO).<sup>45</sup> The FECO fringes were then used to determine the surface separation, surface geometry, deformations and the contact area in-situ and in real time. The silver coated mica sheets were glued onto cylindrical silica disks (radius  $R = 2$  cm) before mounting in the SFA chamber in a cross-cylinder orientation, which is equivalent to the interaction between a sphere of radius  $R$  and a flat surface when  $R$  is much larger than the separation  $D$  as is the case in the present study. The measured force  $F(D)$  between the two curved surfaces can be correlated to the interaction energy per unit area between two flat surfaces,  $W(D)$  using the Derjaguin approximation.<sup>43,46</sup>

The adhesion energy per unit area between two surfaces,  $W_{ad}$ , can be determined from the pull-off force,  $F_{ad}$  (the force required to separate the surfaces from adhesive contact), given by:<sup>43,45-47</sup>

$$W_{ad} = F_{ad}/1.5\pi R \quad (1)$$

In each set of measurements the reference distance ( $D = 0$ ) was determined at the adhesive contact between the two mica surfaces in air prior to introducing the solvents. For the force measurements, ~100  $\mu$ L of desired solvent/solution was injected between two closely placed mica surfaces in the SFA chamber. The chamber was sealed and saturated with the vapor of the same solvent. All experiments were conducted at ambient conditions. During a typical force measurement the two mica surfaces were brought close to each other for an initial approach until the two surfaces do not move any closer, followed by separation of the two surfaces. In this way we obtained the normal force-distance ( $F$  vs.  $D$ ) profile. The “confined film thickness” is defined as the mica-mica separation distance or thickness of confined asphaltenes/EC films which remained almost constant and independent of the applied normal load.

**Topographical Imaging:** Topographical images of treated mica surfaces were obtained using an Agilent 5500 Molecular Imaging Atomic Force Microscope (AFM) (Keysight Technologies Inc., Chandler, AZ). Images were captured using silicon nitride cantilevers (Bruker, Camarillo, CA) operating under AC mode in air at ambient condition. The cantilever nominal resonance frequency was 300-500 kHz, and the amplitude setpoint ( $A_s$ ) was 98% of the free amplitude ( $A_0$ ) in order to apply a very low force on the sample and avoid surface damage during the scanning of the surfaces. Multiple locations were imaged for each substrate and a representative image was then selected.

Sample properties such as root mean square (RMS) roughness, average height and maximum height (pit-to-peak) were calculated for each topographical image using the Pico Image post processing software of Agilent 5500 AFM. The RMS and height values were obtained using the lowest point or zero-plane on the selected image as the reference, as it is not possible to confirm directly from the AFM image that the lowest point is the underlying mica. Considering that freshly-cleaved mica is atomically smooth, the actual height/thickness of the adsorbed layer

would be greater than the reported values if there is any deviation in the layer thickness, provided that the lowest part of the image is mica covered with materials of very uniform features.

## RESULTS AND DISCUSSION

We have previously studied the surface interactions of immobilized and adsorbed asphaltene films in toluene and heptane, and the adsorption of asphaltenes on hydrophilic solid (mica) surface.<sup>37,38</sup> In pure toluene (good solvent), the asphaltene layers were observed to swell by up to 60%, giving rise to large steric repulsion as the two layers approached each other.<sup>48</sup> During retraction of the two surfaces, interpenetration of the swollen asphaltene layers results in weak adhesion  $F_{ad}/R \approx -1 \text{ mN/m}$ , which increases to  $F_{ad}/R \approx -3 \text{ mN/m}$  when the asphaltene layers were immersed in heptane (poor solvent). In heptane the asphaltene molecules readily self-associate as identified by a weak attractive force during approach of the two asphaltene layers. The interaction forces for both immobilized and adsorbed layers were shown to be equivalent, and the adsorption study confirmed diffusion-limited dynamics of asphaltene adsorption on mica.

**Topography of sample surfaces.** The topographical features of asphaltenes and EC layers immobilized on mica surfaces were imaged in air by an AFM operating in tapping mode. As shown in Figure 2a, the AFM image of bare mica showed a featureless flat surface, with a RMS roughness of  $\sim 0.22 \text{ nm}$ . The AFM image of EC and asphaltene layers immobilized on mica are shown in Figures 2b and 2c, respectively. The morphology EC layers appears more uniform and flatter with an average RMS roughness of  $\sim 0.9 \text{ nm}$ , compared with the immobilized asphaltenes which form closely packed nanoaggregates,<sup>37,38</sup> with an average RMS roughness of  $\sim 1.2 \text{ nm}$ .

**Adsorption of Ethyl Cellulose on Mica.** The force-distance profile between two mica surfaces following the injection of 0.5 wt% EC-in-toluene solution is shown in Figure 3a. The force-distance profile was measured at  $t = 5 \text{ min}$  and confirms the fast adsorption of EC macromolecules onto the mica surface. A repulsive force was measured during approach at a separation distance of  $\sim 30 \text{ nm}$  with a confined layer thickness increased from  $0 \text{ nm}$  to  $\sim 14 \text{ nm}$ ,

which corresponds to an  $\sim 7$  nm thickness of the EC layer on each mica surface. Since the electrical double-layer forces in toluene can be considered negligible, repulsive forces observed during the approach of the surfaces are attributed to steric repulsion of solvated macromolecule EC layers. The long-ranged repulsion is suggestive of diffuse trains and loops of EC macromolecules which under compression deform to a more uniform thickness.

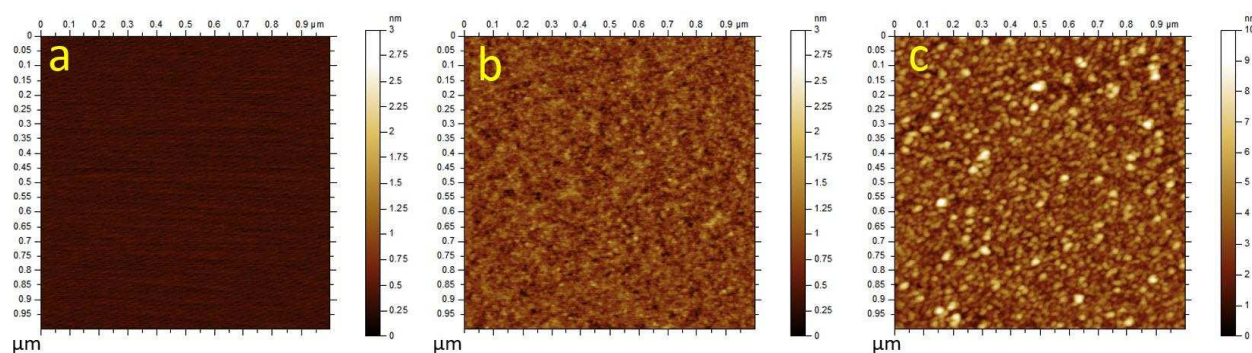


**Figure 2.** Topographic AFM images of (a) bare mica surface, (b) immobilized EC layer on mica surface in air, and (c) immobilized asphaltene layer on mica surface imaged in air. Note that the surfaces were gently dried with nitrogen before imaging.

The retraction force-distance profile in Figure 3a shows an adhesion of  $F_{ad}/R \approx -1$  mN/m, most likely due to the interpenetration of EC macromolecules on the two opposing surfaces in contact, as also evident from the stretching behavior shown in the force profile before the two surfaces finally detached.

**Interaction between asphaltenes and EC immobilized surfaces in toluene.** The intermolecular forces of asphaltenes and EC immobilized on mica were measured in toluene using SFA in an asymmetrical configuration as shown in the inset of Figure 3b. The experimental set up consists of an asphaltene layer coated on one mica surface interacting with the EC layer coated on the other mica surface.

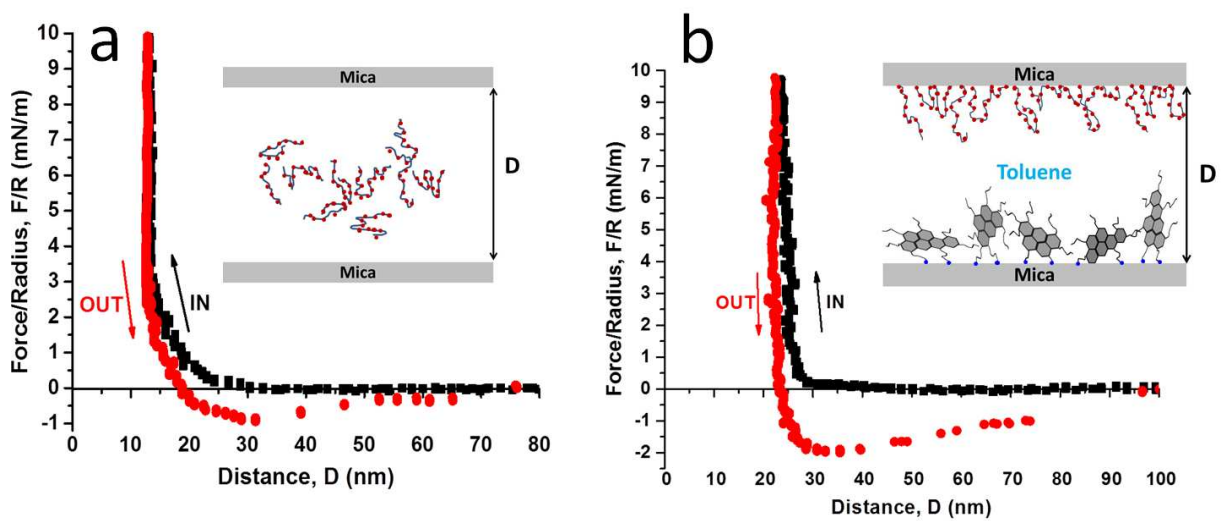


**Figure 3.** Force-distance profiles: (a) between two bare mica surfaces after ~5 min immersion in 0.5 wt% EC-in-toluene solution, and (b) between EC and asphaltene layers immobilized on mica (asymmetric surfaces). In this figure and all subsequent figures, “In” indicates approach of the two surfaces and “Out” indicates separation of the two surfaces.

Figure 3b shows the force-distance profile measured after exposing the two immobilized layers (EC and asphaltene) in toluene for ~10 min. As the two surfaces were brought into contact, a repulsive force was measured at ~35 nm with a confined layer thickness of ~23 nm. The repulsive force measured during approach of the two layers in toluene is attributed to steric repulsion of swollen asphaltenes and EC layers. Strong adhesion ( $F_{ad}/R \approx -2 \text{ mN/m}$ ;  $W_{ad} = 0.42 \text{ mJ/m}^2$ ) was measured during separation and is most likely due to interpenetration of asphaltenes and EC macromolecules under the applied load. Interestingly, the adhesion for the asymmetric system (EC/asphaltene-in-toluene) is stronger than the adhesion between asphaltene-asphaltene and EC-EC layers in toluene. Considering good solvency of EC macromolecules in toluene and core-branched structure of asphaltenes, it is likely that the stronger adhesion results from: i) increased interpenetration and tangling of EC macromolecules and asphaltene aliphatic branches, and ii) bridging adhesion as immobilized EC and asphaltene layers interact with opposing surfaces at short separation distances, see Figure 4c for schematic representation of likely molecular interactions.

Toluene is a good solvent for both asphaltenes and EC, hence the hydrocarbon chains of the immobilized asphaltenes and EC molecules on mica surface tend to stretch and act as a swollen brush. Therefore, the steric repulsion between these two layers can be pseudo-quantitatively described by the Alexander–de Gennes (AdG) model developed originally for two interacting polymer brush layers.<sup>49-51</sup> When two polymer brush surfaces approach each other, the brush layers at some distance start to overlap, leading to an increase in the local density of “polymer segments”. This in turn leads to a sharp increase in osmotic pressure and repulsive interaction energy. The repulsive pressure between two planar layers is given by:<sup>49-52</sup>

$$P(D) \approx \frac{kT}{s^3} \left[ \left( \frac{2L}{D} \right)^{\frac{9}{4}} - \left( \frac{D}{2L} \right)^{\frac{3}{4}} \right] \text{ for } D < 2L \quad (2)$$

where  $s$  is the mean distance between anchoring (or grafting) sites on the surface,  $L$  is the brush layer thickness per surface,  $T$  is the temperature, and  $k$  is the Boltzmann constant. For the geometry of two crossed cylinders of radius  $R$  (used in our experiments), the force between them is given by first integrating the above equation and then using the Derjaguin approximation as:<sup>49-52</sup>

$$\frac{F(D)}{R} = 2\pi \int P(D) dD = \frac{16\pi kTL}{35s^3} \left[ 7 \left( \frac{2L}{D} \right)^{5/4} + 5 \left( \frac{D}{2L} \right)^{7/4} - 12 \right] \quad (3)$$

The AdG model fittings of the measured repulsive forces for EC-in-toluene and for the asymmetric system of asphaltenes/EC-in-toluene are shown in Figures 4a and 4b, respectively. Comparing Figures 4a and 4b, it is evident that a single set of parameters can describe the force profile of EC-in-toluene in both the low compression and high compression regimes. This good fit of single set of parameter illustrates that the EC macromolecules exhibit classical polymer behavior. However, for the asphaltenes-EC system at larger separation distances under lower compression force, deviation is observed between the experimental data and the single parameter AdG model fit. We have previously shown that for asphaltenes-in-toluene<sup>38</sup> in the low compression region a second set of parameters is necessary to fit the experimental data using the AdG model, indicating the presence of secondary structures. A second set of fitting parameters

seems reasonable when considering the complex molecular structure of asphaltenes, which includes a polyaromatic core of several aromatic rings, branched aliphatic side chains, and an ability to self-associate to form nanoaggregates (asphaltene polydispersity). An independent set of parameters have been used to fit the data in the low compression region as shown in Figure 4b (dashed line). The fitted parameters of  $s$  and  $L$  are listed in Table 1.

For the asymmetric system (asphaltene/EC-in-toluene) the brush layer thickness equalled 14.6 nm. To determine the relative thickness of each layer a comparative study of asphaltene-mica and EC-mica was conducted. As anticipated, the summation of each individual layer thickness approximates to the layer thickness of the asymmetric film ( $2L_{Asp} + 2L_{EC} = 2L_{Asp/EC}$ ). Hence, for the asphaltene-EC asymmetric layers, the thickness of the asphaltene layer is greater than the thickness of the EC layer. It is also worth noting that the thickness of the EC-mica and asphaltene-mica layer is equivalent to half the brush layer thickness of symmetrical EC and asphaltene layers, demonstrating good reproducibility when forming immobilized layers.

**Asphaltene immobilized substrates and EC solution.** The experimental setup to measure the intermolecular forces of immobilized asphaltene layers in EC-in-toluene solution using a SFA is shown in the inset of Figure 5a. Force-distance profiles of asphaltene immobilized on mica surfaces in 0.5 wt% EC-in-toluene solution at different time intervals are shown in Figure 5a. In the absence of EC the confined layer thickness for asphaltene layers on mica immersed in toluene was equal to ~18 nm (solid line, Figure 5a). Following the addition of 0.5 wt% EC-in-toluene solution, long-range repulsion was measured on approach with a confined layer thickness under high loading force equal to ~30 nm. Growth in the confined layer thickness from 18 nm to 30 nm occurs within the first 5 min, with little variation in the confined layer thickness thereafter (i.e. from 30 to 280 min). The result suggests that modification of the asphaltene layers in the presence of EC macromolecules is rapid, with negligible long time dependence. Little variation in the confined layer thickness is also confirmed by similar force curves on retraction as shown in Figure 5b. While the pull-off force distance extended by 150 nm without abrupt jump-apart, representing a significant stretching of the interacting interfacial layers in the presence of EC, the

adhesion energy is seen to decrease slightly from  $\sim 0.51 \text{ mJ/m}^2$  to  $\sim 0.42 \text{ mJ/m}^2$  as shown in the inset of Figure 5b. The interaction mechanism between asphaltene layer and EC molecules is further investigated by using in situ AFM imaging and discussed below.

**Table 1.** Fitting Parameters to the AdG Scaling Model

Asphaltene and EC surfaces in toluene			EC surfaces in toluene			
At $\sim 10$ min	High Loading <sup>a</sup>		Low Loading <sup>b</sup>		At $\sim 10$ min	
2L (nm)	14.6		19.0		10.5	
S (nm)	2.0		6.9		4.3	
	A-A <sup>c</sup>		A-M <sup>c</sup>		E-E	E-M
	High L	Low L	High L	Low L		
2L (nm)	17.6	33.0	8.8	16.5		
S (nm)	2.8	12.5	2.8	12.5	4.3	4.3

A: asphaltene, E: ethyl-cellulose, M: mica. <sup>a</sup> High compression and short separation distance regime (solid fitting curve). <sup>b</sup> Low compression and long separation distance regime (dash fitting curve). <sup>c</sup> Previously published results.<sup>38</sup>

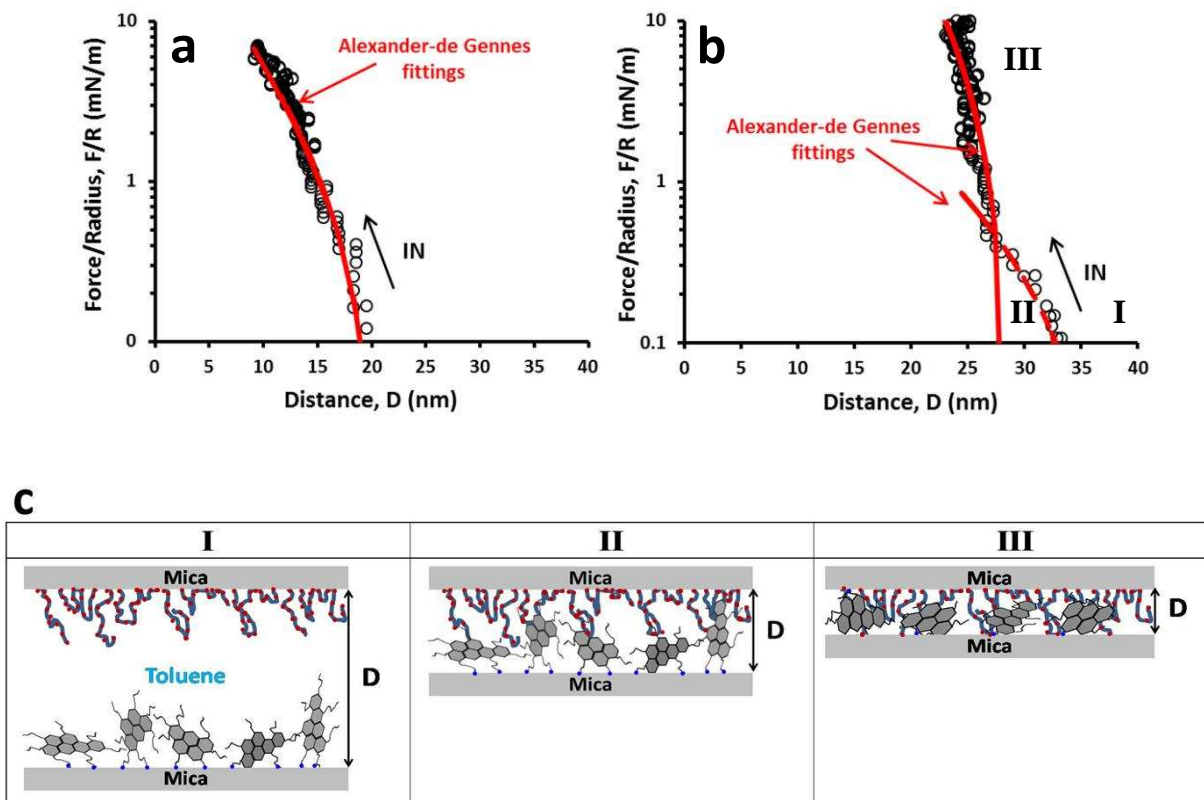


**Figure 4.** Experimentally measured repulsive forces and the best fitted curves of the force profiles with the AdG theory for approach of (a) EC layers in toluene and (b) asphaltene layer against an EC layer in toluene, with schematics (c) of the likely interactions between asphaltenes and EC molecules as the two immobilized layers move into contact and deform under high loading force: **I** – large separation distance between the two surfaces and no measurable interaction force; **II** – long range steric repulsion as the solvated EC molecules begin to interact with the aliphatic branches of the solvated asphaltene molecules; and **III** – strong steric repulsion as the EC molecules and asphaltene polyaromatic core resist the high normal loading force (condition of the confined layer thickness).

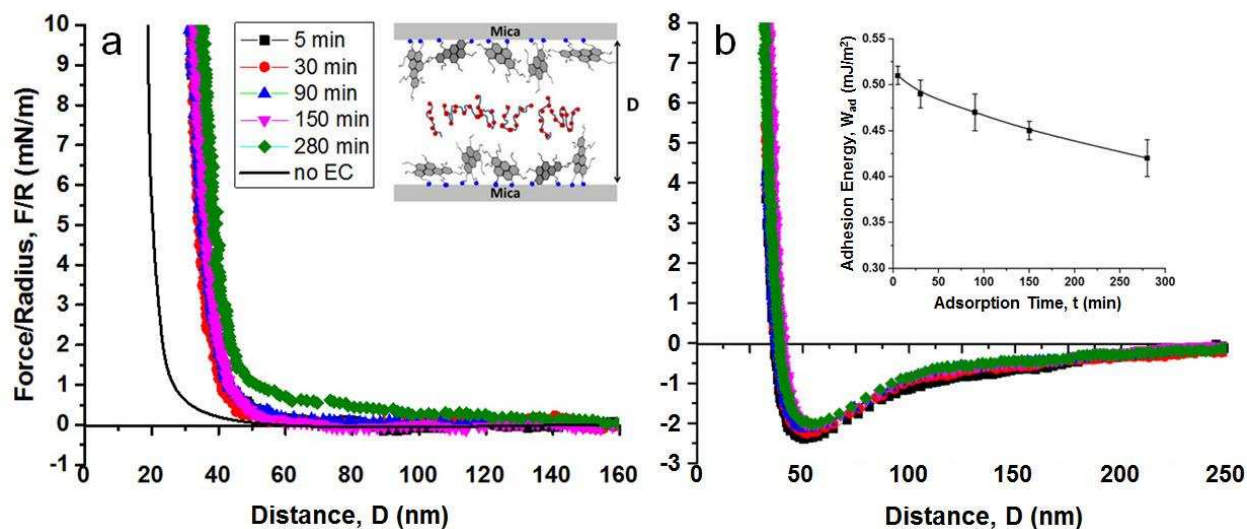


**Figure 5.** (a) Approach force profiles of two asphaltenes layers in EC-toluene solution at different time intervals (inset – schematic demonstrating the experimental setup); (b) Separation force profiles of two asphaltenes layers in EC-toluene solution at different time intervals. Inset: Adhesion energy,  $W_{ad}$ , between asphaltenes immobilized surfaces in EC-toluene solution as a function of time at 24°C.

Structural differences between asphaltenes and EC layers immobilized on mica are shown by the AFM images in Figure 2, where asphaltenes form randomly distributed nanoaggregates and EC molecules form a uniform and flatter layer on the mica surface. Surface topography of the adsorbed asphaltene layer as a function of immersion time in EC-in-toluene solution is shown in Figure 6. Freshly cleaved mica was first immersed in 0.5 wt% asphaltene-in-toluene solution for 30 min to form adsorbed asphaltene layer. The surface was then rinsed with copious amounts of toluene to remove any loosely attached asphaltenes, and subsequently immersed in 0.5 wt% EC-in-toluene solution for variable periods of time between 5 and 240 min. At the desired immersion time in EC solution, the substrate was gently removed and rinsed with toluene before drying using nitrogen. With increasing immersion time the surface topography of asphaltene layer on mica showed two distinct changes: i) asphaltene nanoaggregates were observed to grow rapidly (within 5 min); and ii) discrete flat areas on the mica substrate continually expanded. Figures 6b, 6c and 6d clearly depict these larger rough domains (large globule structures/aggregates) and

much expanded flat open areas. The substrate RMS roughness at 240 min immersion time is almost equivalent to the RMS of EC immobilized layer on mica (comparing Figures 2b and 6d). The observed topography change suggests that EC macromolecules displaced asphaltenes which form larger globule structures/aggregates. The AFM image height profiles show a relative height of asphaltene aggregates on the mica/EC surface to be  $\sim 15$  nm. The confined layer thickness from the SFA force curve in Figure 5a is  $\sim 30$  nm, which is equivalent to a  $\sim 15$  nm “layer” on each surface, confirming our displacement hypothesis of immobilized asphaltene layers by competitive adsorption of EC macromolecules.

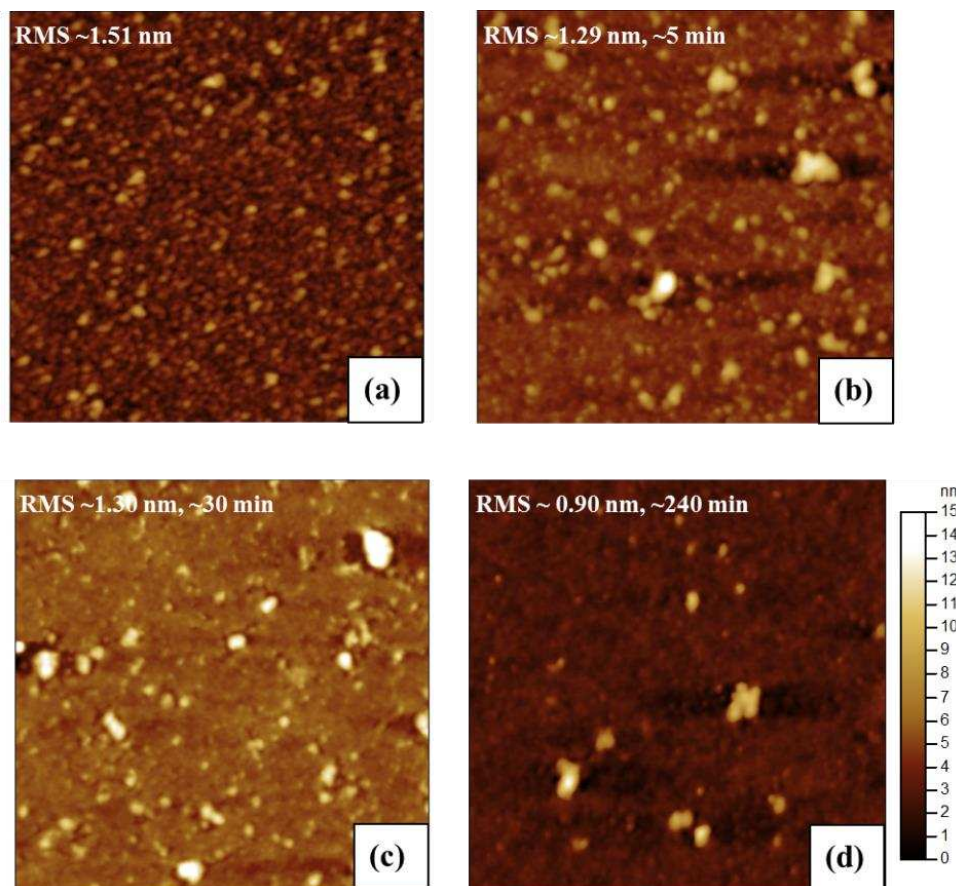


**Figure 6.** AFM topography images of asphaltene layers immobilized on mica and immersed in 0.5 wt% EC-in-toluene solution for different times. (a) Asphaltenes adsorbed on mica surface in pure toluene (without EC). (b), (c) and (d) Following immersion of (a) in EC solution for  $\sim 5$  min,  $\sim 30$  min and  $\sim 240$  min, respectively. The dimension of images is  $1 \mu\text{m} \times 1 \mu\text{m}$ .

As seen from the AFM images, the displacement of asphaltenes on the mica surface correlates with the measured force profiles in Figure 5a. The larger globule structures of asphaltenes following 5 min immersion of the immobilized asphaltene layers in EC-in-toluene solution contribute to the increase in long range repulsive force as observed in Figure 5a. In addition, the time-dependent adhesion energy between the two surfaces reduced by approximately ~20% from  $\sim 0.51 \text{ mJ/m}^2$  to  $\sim 0.42 \text{ mJ/m}^2$  after 280 min of immersion, see Figure 5b. The slight reduction in the adhesion energy correlates to a reduced number of asphaltene clusters interacting between the two surfaces, as shown by Figure 6d. However, the dominant interaction between the two surfaces at all immersion times is asphaltene-asphaltene, since the EC macromolecules displace asphaltenes which form large globules/nanoaggregates. These large globules/nanoaggregates protrude out from the underlying substrate to dominate the surface-surface interactions. It is worth reiterating that EC adsorption on mica does not promote the detachment of asphaltene molecules (re-solvate into the organic phase), but the self-association of asphaltenes to form large clusters.

## CONCLUSION

The interaction forces between EC and asphaltene layers immobilized on mica were measured using SFA, and AFM was used as a complimentary technique to provide visual assessment of layer topography. With all studies conducted in a non-aqueous environment, strong repulsion between symmetrical (EC-EC, asphaltene-asphaltene) and asymmetrical (EC-asphaltene) surfaces was attributed to steric hindrance of swollen asphaltene and EC layers. Under compression (high normal force) the interacting layers exhibited pull-off adhesion due to interpenetration of neighboring molecules.

A time-dependent study was considered to elucidate the interaction between immobilized asphaltene layers immersed in EC-in-toluene solution (mimicking demulsification of W/O emulsions). Following the addition of EC solution a rapid change in the confined layer thickness was measured (less than 5 min), although the confined layer thickness showed little variance thereafter. The adhesion energy between the two interacting surfaces gradually reduced by ~20% and this was attributed to a decrease in the number of asphaltene-asphaltene contacts. Further

analysis by AFM confirmed the rapid expansion of EC macromolecules on the mica surface, displacing the immobilized asphaltene layer, with asphaltene molecules self-associating to form larger clusters within an EC dominated film. Since the interaction between EC macromolecules and asphaltenes is purely repulsive, displacement of asphaltenes occurred due to the higher number of hydroxyl groups per EC macromolecule, leading to a stronger binding affinity of EC on the hydrophilic mica surface.

The enhanced stability of water-in-crude oil emulsions is frequently attributed to the formation of asphaltene interfacial layers that inhibit droplet coalescence. Separation can be improved by adding demulsifiers which disrupt the asphaltene network. This is the first study to measure the interaction forces between asphaltenes and demulsifier molecules, elucidating the asphaltene displacement mechanism. While the effectiveness of EC as a water-in-crude oil demulsifier has previously been demonstrated, this study confirmed that asphaltenes displacement and network disruption can occur through the addition of demulsifier molecules. The long-range repulsion measured during approach between asphaltene layers contributes to the stabilization of interfacial layers and water-in-oil emulsions. While the adhesion measured after the addition of EC molecules indicate that EC molecules can be interfacially active to penetrate into the interfacial asphaltene layers, contributing to the adhesion measured. Both AFM imaging and SFA force measurements suggest that the EC demulsifier molecules exhibit strong affinity to hydrophilic mineral surfaces (i.e. mica), penetrating the pre-formed asphaltene layers to break-up the asphaltene network. Such penetration is possible as a result of aliphatic side chains (containing polar functional groups and heteroatoms) of asphaltenes that prevent their close packing. In contrast, the polar (e.g. hydroxyl) groups on EC molecules are more populated and uniformly distributed along their polymeric chains. As a result, each EC molecule can form multiple attractive bonds with the oil-water or oil-solid interface. Once adsorbed, the EC molecules are likely to spread and gradually expand to compete for more binding sites at the interface, changing the aggregation state of the asphaltenes at the interface and thus facilitating the demulsification process. This fundamental insight can be used to design better, smarter chemicals for more effective demulsification performance.

## ACKNOWLEDGMENT

Hongbo Zeng acknowledges the Natural Sciences and Engineering Research Council of Canada (NSERC), Petro-Canada Young Innovator Award and Suncor Energy Inc for the support of the work. The authors also acknowledge the NSERC Industrial Research Chair Program in Oil Sands Engineering (held by Zhenghe Xu) for the support of the study. Thanks are due to Syncrude Canada Ltd. for providing the bitumen samples.

## REFERENCES

1. Masliyah, J.; Zhou, Z.; Xu, Z.; Czarnecki, J.; Hamza, H., Understanding water-based bitumen extraction from athabasca oil sands. *Can. J. Chem. Eng.* **2004**, 82 (4), 628-654.
2. Czarnecki, J. In *Stabilization of water in crude oil emulsions. part 2*, 2009; American Chemical Society: pp 1253-1257.
3. Wu, X., Investigating the Stability Mechanism of Water-in-Diluted Bitumen Emulsions through Isolation and Characterization of the Stabilizing Materials at the Interface. *Energy & Fuels* **2003**, 17 (1), 179-190.
4. Ivanova, N. O.; Xu, Z.; Liu, Q.; Masliyah, J. H., Surface Forces in Unconventional Oil Processing. *Curr. Opin. Colloid Interface Sci.*, DOI: 10.1016/j.cocis.2016.09.013.
5. Zhang, L.; Shi, C.; Lu, Q. G.; Liu, Q. X.; Zeng, H. B., Probing Molecular Interactions of Asphaltenes in Heptol Using a Surface Forces Apparatus: Implications on Stability of Water-in-Oil Emulsions. *Langmuir* **2016**, 32 (19), 4886-4895.
6. Shi, C.; Zhang, L.; Xie, L.; Lu, X.; Liu, Q. X.; Mantilla, C. A.; van den Berg, F. G. A.; Zeng, H. B., Interaction Mechanism of Oil-in-Water Emulsions with Asphaltenes Determined Using Droplet Probe AFM. *Langmuir* **2016**, 32 (10), 2302-2310.
7. Sparks, B. D.; Kotlyar, L. S.; O'Carroll, J. B.; Chung, K. H., Athabasca oil sands: Effect of organic coated solids on bitumen recovery and quality. *J. Pet. Sci. Eng.* **2003**, 39 (3-4), 417-430.
8. Kotlyar, L. S.; Sparks, B. D.; Woods, J. R.; Chung, K. H., Solids associated with the asphaltene fraction of oil sands bitumen. *Energy & Fuels* **1999**, 13 (2), 346-350.
9. Yeung, A.; Dabros, T.; Masliyah, J.; Czarnecki, J., Micropipette: A new technique in emulsion research. *Colloids Surf., A* **2000**, 174 (1-2), 169-181.

10. Czarnecki, J.; Tchoukov, P.; Dabros, T., Possible role of asphaltenes in the stabilization of water-in-crude oil emulsions. *Energy & Fuels* **2012**, 26 (9), 5782-5786.
11. Tchoukov, P.; Yang, F.; Xu, Z.; Dabros, T.; Czarnecki, J.; Sjoblom, J., Role of asphaltenes in stabilizing thin liquid emulsion films. *Langmuir* **2014**, 30 (11), 3024-3033.
12. Langevin, D.; Argillier, J.-F., Interfacial behavior of asphaltenes. *Adv. Colloid Interface Sci.*, DOI: 10.1016/j.cis.2015.10.005.
13. Spiecker, P. M.; Kilpatrick, P. K., Interfacial rheology of petroleum asphaltenes at the oil-water interface. *Langmuir* **2004**, 20 (10), 4022-4032.
14. Pauchard, V.; Rane, J. P.; Banerjee, S., Asphaltene-laden interfaces form soft glassy layers in contraction experiments: A mechanism for coalescence blocking. *Langmuir* **2014**, 30 (43), 12795-12803.
15. Harbottle, D.; Chen, Q.; Moorthy, K.; Wang, L.; Xu, S.; Liu, Q.; Sjoblom, J.; Xu, Z., Problematic stabilizing films in petroleum emulsions: Shear rheological response of viscoelastic asphaltene films and the effect on drop coalescence. *Langmuir* **2014**, 30 (23), 6730-6738.
16. Rane, J. P.; Pauchard, V.; Couzis, A.; Banerjee, S., Interfacial rheology of asphaltenes at oil-water interfaces and interpretation of the equation of state. *Langmuir* **2013**, 29 (15), 4750-4759.
17. Yarranton, H. W.; Sztukowski, D. M.; Urrutia, P., Effect of interfacial rheology on model emulsion coalescence. I. Interfacial rheology. *J. Colloid Interface Sci.* **2007**, 310 (1), 246-252.
18. Gu, G.; Zhang, L.; Wu, X. A.; Xu, Z.; Masliyah, J., Isolation and characterization of interfacial materials in bitumen emulsions. *Energy & Fuels* **2006**, 20 (2), 673-681.
19. Czarnecki, J.; Moran, K.; Yang, X., On the "rag layer" and diluted bitumen froth dewatering. *Can. J. Chem. Eng.* **2007**, 85 (5), 748-755.
20. Feng, X.; Mussone, P.; Gao, S.; Wang, S.; Wu, S.-Y.; Masliyah, J. H.; Xu, Z., Mechanistic study on demulsification of water-in-diluted bitumen emulsions by ethylcellulose. *Langmuir* **2010**, 26 (5), 3050-3057.
21. Pensini, E.; Harbottle, D.; Yang, F.; Tchoukov, P.; Li, Z.; Kailey, I.; Behles, J.; Masliyah, J.; Xu, Z., Demulsification mechanism of asphaltene-stabilized water-in-oil emulsions by a

- polymeric ethylene oxide-propylene oxide demulsifier. *Energy & Fuels* **2014**, 28 (11), 6760-6771.
22. Hou, J.; Feng, X.; Masliyah, J.; Xu, Z., Understanding interfacial behavior of ethylcellulose at the water-diluted bitumen interface. *Energy & Fuels* **2012**, 26 (3), 1740-1745.
  23. Feng, X.; Wang, S.; Hou, J.; Wang, L.; Cepuch, C.; Masliyah, J.; Xu, Z., Effect of hydroxyl content and molecular weight of biodegradable ethylcellulose on demulsification of water-in-diluted bitumen emulsions. *Ind. Eng. Chem. Res.* **2011**, 50 (10), 6347-6354.
  24. Fan, Y.; Simon, S.; Sjöblom, J., Chemical destabilization of crude oil emulsions: Effect of nonionic surfactants as emulsion inhibitors. *Energy & Fuels* **2009**, 23 (9), 4575-4583.
  25. Feng, X.; Xu, Z.; Masliyah, J., Biodegradable polymer for demulsification of water-in-bitumen emulsions. *Energy & Fuels* **2009**, 23 (1), 451-456.
  26. Zaki, N. N.; Abdel-Raouf, M. E.; Abdel-Azim, A. A. A., Propylene Oxide-Ethylene Oxide Block Copolymers as Demulsifiers for Water-in-Oil Emulsions, II [1]. Effects of Temperature, Salinity, pH-Value, and Solvents on the Demulsification Efficiency. *Monatsh. Chem.* **1996**, 127 (12), 1239-1245.
  27. Wu, J.; Xu, Y.; Dabros, T.; Hamza, H., Effect of EO and PO positions in nonionic surfactants on surfactant properties and demulsification performance. *Colloids Surf., A* **2005**, 252 (1), 79-85.
  28. Kim, Y.-H.; Nikolov, A. D.; Wasan, D. T.; Diaz-Arauzo, H.; Shelly, C. S., Demulsification of water-in-crude oil emulsions: effects of film tension, elasticity, diffusivity and interfacial activity of demulsifier individual components and their blends. *J. Dispersion Sci. Technol.* **1996**, 17 (1), 33-53.
  29. Gong, C.; Towner, J. W., Study of Dynamic Interfacial Tension for Demulsification of Crude Oil Emulsions. Paper presented at SPE 2001: International Symposium on Oilfield Chemistry February 13-16, **2001**, Houston, Texas.
  30. Al-Sabagh, A. M.; Kandile, N. G.; Noor El-Din, M. R., Functions of Demulsifiers in the Petroleum Industry. *Sep. Sci. Technol.* **2011**, 46 (7), 1144-1163.
  31. Pradilla, D.; Simon, S.; Sjöblom, J., Mixed Interfaces of Asphaltenes and Model Demulsifiers, Part II: Study of Desorption Mechanisms at Liquid/Liquid Interfaces. *Energy & Fuels* **2015**, 29 (9), 5507-5518.

32. Fan, Y.; Simon, S.; Sjöblom, J., Interfacial shear rheology of asphaltenes at oil–water interface and its relation to emulsion stability: Influence of concentration, solvent aromaticity and nonionic surfactant. *Colloids Surf., A* **2010**, 366 (1–3), 120-128.
33. Yang, F., Bitumen fractions responsible for stabilizing water in oil emulsions (Doctoral Dissertation). University of Alberta, 2016.
34. Harbottle, D.; Liang, Y.; Xu, Z. Asphaltene-stabilized emulsions: an interfacial rheology study. Paper presented at IBEREO 2015: Challenges in rheology and product development September 9-11, **2015**, Coimbra, Portugal.
35. Wang, S.; Segin, N.; Wang, K.; Masliyah, J. H.; Xu, Z., Wettability control mechanism of highly contaminated hydrophilic silica/alumina surfaces by ethyl cellulose. *J. Phys. Chem. C* **2011**, 115 (21), 10576-10587.
36. Pradilla, D.; Subramanian, S.; Simon, S.; Sjöblom, J.; Beurroies, I.; Denoyel, R., Microcalorimetry Study of the Adsorption of Asphaltenes and Asphaltene Model Compounds at the Liquid–Solid Surface. *Langmuir* **2016**, 32 (29), 7294-7305.
37. Natarajan, A.; Kuznicki, N.; Harbottle, D.; Masliyah, J.; Zeng, H.; Xu, Z., Understanding mechanisms of asphaltene adsorption from organic solvent on mica. *Langmuir* **2014**, 30 (31), 9370-9377.
38. Natarajan, A.; Xie, J.; Wang, S.; Masliyah, J.; Zeng, H.; Xu, Z., Understanding molecular interactions of asphaltenes in organic solvents using a surface force apparatus. *J. Phys. Chem. C* **2011**, 115 (32), 16043-16051.
39. Kupai, M. M.; Yang, F.; Harbottle, D.; Moran, K.; Masliyah, J.; Xu, Z., Characterising rag-forming solids. *Can. J. Chem. Eng.* **2013**, 91 (8), 1395-1401.
40. Yang, F.; Tchoukov, P.; Pensini, E.; Dabros, T.; Czarnecki, J.; Masliyah, J.; Xu, Z., Asphaltene subfractions responsible for stabilizing water-in-crude oil emulsions. Part 1: Interfacial behaviors. *Energy & Fuels* **2014**, 28 (11), 6897-6904.
41. Yang, F.; Tchoukov, P.; Dettman, H.; Teklebrhan, R. B.; Liu, L.; Dabros, T.; Czarnecki, J.; Masliyah, J.; Xu, Z., Asphaltene Subfractions Responsible for Stabilizing Water-in-Crude Oil Emulsions. Part 2: Molecular Representations and Molecular Dynamics Simulations. *Energy & Fuels* **2015**, 29 (8), 4783-4794.

42. Subramanian, S.; Simon, S.; Gao, B.; Sjöblom, J., Asphaltene fractionation based on adsorption onto calcium carbonate: Part 1. Characterization of sub-fractions and QCM-D measurements. *Colloids Surf., A* **2016**, 495, 136-148.
43. Israelachvili, J. N., Intermolecular and surface forces / Jacob N. Israelachvili. Academic Press: London ; San Diego, 1991.
44. Israelachvili, J.; Min, Y.; Akbulut, M.; Alig, A.; Carver, G.; Greene, W.; Kristiansen, K.; Meyer, E.; Pesika, N.; Rosenberg, K.; Zeng, H., Recent advances in the surface forces apparatus (SFA) technique. *Rep. Prog. Phys.* **2010**, 73 (3).
45. Israelachvili, J. N., Thin film studies using multiple-beam interferometry. *J. Colloid Interface Sci.* **1973**, 44 (2), 259-272.
46. Akbulut, M.; Alig, A. R. G.; Min, Y.; Belman, N.; Reynolds, M.; Golan, Y.; Israelachvili, J., Forces between Surfaces across Nanoparticle Solutions: Role of Size, Shape, and Concentration. *Langmuir* **2007**, 23 (7), 3961-3969.
47. Zeng, H. B.; Maeda, N.; Chen, N. H.; Tirrell, M.; Israelachvili, J., Adhesion and friction of polystyrene surfaces around Tg. *Macromolecules* **2006**, 39 (6), 2350-2363.
48. Wang, S.; Liu, J.; Zhang, L.; Masliyah, J.; Xu, Z., Interaction forces between asphaltene surfaces in organic solvents. *Langmuir* **2010**, 26 (1), 183-190.
49. de Gennes, P. G., Polymers at an interface: a simplified view. *Adv. Colloid Interface Sci.* **1987**, 27 (3-4), 189-209.
50. Kuhl, T. L.; Leckband, D. E.; Lasic, D. D.; Israelachvili, J. N., Modulation of interaction forces between bilayers exposing short-chained ethylene oxide headgroups. *Biophys. J.* **1994**, 66 (5), 1479-1488.
51. Butt, H.-J.; Kappl, M.; Mueller, H.; Raiteri, R.; Meyer, W.; Rühle, J., Steric Forces Measured with the Atomic Force Microscope at Various Temperatures. *Langmuir* **1999**, 15 (7), 2559-2565.
52. Zhang, L.; Zeng, H. B.; Liu, Q. X., Probing Molecular and Surface Interactions of Comb-Type Polymer Polystyrene-graft-poly(ethylene oxide) (PS-g-PEO) with an SFA. *J. Phys. Chem. C* **2012**, 116 (33), 17554-17562.

Table of Content (TOC) image

